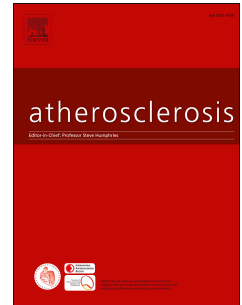


# Journal Pre-proof

TIGAR mitigates atherosclerosis by promoting cholesterol efflux from macrophages

Zhen-Wang Zhao, Min Zhang, Jin Zou, Xiang-Jun Wan, Li Zhou, Yao Wu, Shang-Ming Liu, Ling-Xiao Liao, Heng Li, Yu-Sheng Qin, Xiao-Hua Yu, Chao-Ke Tang



PII: S0021-9150(21)00179-9

DOI: <https://doi.org/10.1016/j.atherosclerosis.2021.04.002>

Reference: ATH 16601

To appear in: *Atherosclerosis*

Received Date: 20 September 2020

Revised Date: 8 March 2021

Accepted Date: 9 April 2021

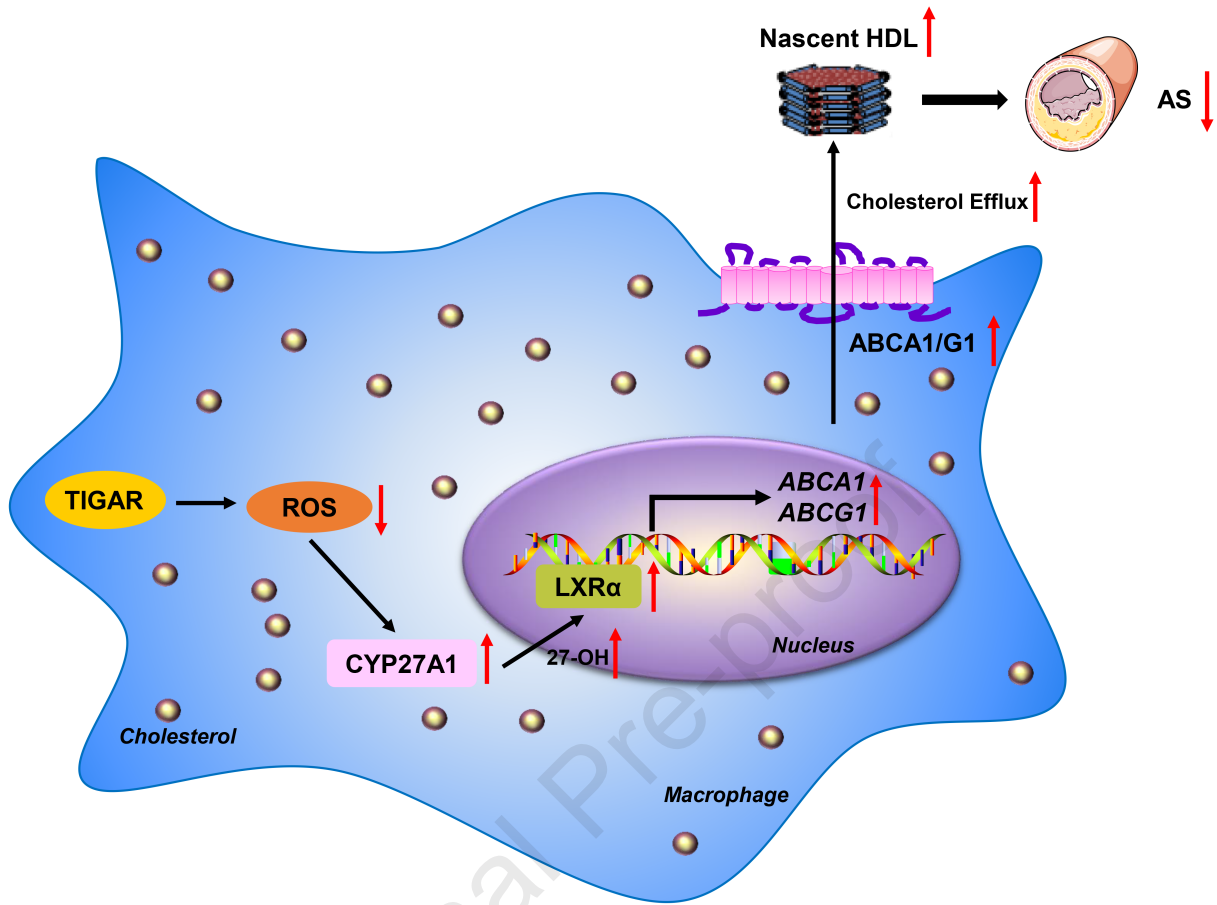
Please cite this article as: Zhao Z-W, Zhang M, Zou J, Wan X-J, Zhou L, Wu Y, Liu S-M, Liao L-X, Li H, Qin Y-S, Yu X-H, Tang C-K, TIGAR mitigates atherosclerosis by promoting cholesterol efflux from macrophages, *Atherosclerosis*, <https://doi.org/10.1016/j.atherosclerosis.2021.04.002>.

This is a PDF file of an article that has undergone enhancements after acceptance, such as the addition of a cover page and metadata, and formatting for readability, but it is not yet the definitive version of record. This version will undergo additional copyediting, typesetting and review before it is published in its final form, but we are providing this version to give early visibility of the article. Please note that, during the production process, errors may be discovered which could affect the content, and all legal disclaimers that apply to the journal pertain.

© 2021 Elsevier B.V. All rights reserved.

### **Credit Author Statement**

Zhen-Wang Zhao, Min Zhang, Jin Zou, Conception, design, execution of the experiments, analysis and interpretation of data and writing of the initial draft of the manuscript. Xiang-Jun Wan, Li Zhou, Yao Wu, worked with the *Apoe*<sup>-/-</sup> model of atherosclerosis. Shang-Ming Liu, Ling-Xiao Liao, Heng Li, Yu-Sheng Qin, worked with the cell experiment. Xiao-Hua Yu, Chao-Ke Tang, critically evaluated and edited the manuscript. In addition, the Zhen-Wang Zhao, Min Zhang, Xiao-Hua Yu and Chao-Ke Tang modified the manuscripts followed the reviewers' suggestion.



## **TIGAR mitigates atherosclerosis by promoting cholesterol efflux from macrophages**

Zhen-Wang Zhao<sup>1,\*</sup>, Min Zhang<sup>1,\*</sup>, Jin Zou<sup>1,\*</sup>, Xiang-Jun Wan<sup>1</sup>, Li Zhou<sup>1</sup>, Yao Wu<sup>1</sup>, Shang-Ming Liu<sup>1</sup>, Ling-Xiao Liao<sup>1,3</sup>, Heng Li<sup>1</sup>, Yu-Sheng Qin<sup>1</sup>, Xiao-Hua Yu<sup>2,\*\*</sup>, Chao-Ke Tang<sup>1,\*\*</sup>

<sup>1</sup> Institute of Cardiovascular Disease, Key Lab for Arteriosclerosis of Hunan Province, Hunan International Scientific and Technological Cooperation Base of Arteriosclerotic Disease, Hunan Province Cooperative Innovation Center for Molecular Target New Drug Study, Hengyang medical school, University of South China, Hengyang, Hunan 421001, China.

<sup>2</sup> Institute of Clinical Medicine, The Second Affiliated Hospital of Hainan Medical University, Haikou 570100, China.

<sup>3</sup> Institute of Pharmacy & Pharmacology, University of South China, Hengyang, Hunan 421001, China.

\*\* Corresponding author: Xiao-Hua Yu, Ph.D. Institute of Clinical Medicine, The Second Affiliated Hospital of Hainan Medical University, Haikou, Hainan 460106, China. E-mail: [yxh167@qq.com](mailto:yxh167@qq.com).

\*\* Corresponding author: Chao-Ke Tang, PhD, Professor, Institute of Cardiovascular Research, University of South China, Hengyang, Hunan, 421001, China. Email: [tangchaoke@qq.com](mailto:tangchaoke@qq.com). Tel: 86-734-8281853

\* These authors contributed equally to this work

## Abstract

**Background and aims:** TP53-induced glycolysis and apoptosis regulator (TIGAR) is now characterized as a fructose-2,6-bisphosphatase to reduce glycolysis and protect against oxidative stress. Recent studies have demonstrated that TIGAR is associated with cardiovascular disease. However, little is known about its role in atherosclerogenesis. In this study, we aimed to investigate the effect of TIGAR on atherosclerosis and explore the underlying molecular mechanism.

**Methods:** The Gene Expression Omnibus (GEO) datasets were used to analyze the differential expression of relative proteins. THP-1-derived macrophages were used as an *in vitro* model and apolipoprotein E-deficient (*Apoe*<sup>-/-</sup>) mice were used as an *in vivo* model. [<sup>3</sup>H] labeled cholesterol was used to assess the capacity of cholesterol efflux and reverse cholesterol transport (RCT). Both qPCR and Western blot were used to evaluate the mRNA and protein expression, respectively. Lentiviral vectors were used to disturb the expression of TIGAR *in vitro* and *in vivo*. Oil Red O, hematoxylin-eosin, and Masson staining were performed to evaluate atherosclerotic plaques in *Apoe*<sup>-/-</sup> mice fed a Western diet. Conventional assay kits were used to measure the levels of reactive oxygen species (ROS), plasma lipid profiles and 27-hydroxycholesterol (27-HC).

**Results:** Our results showed that TIGAR is increased upon the formation of macrophage foam cells and atherosclerosis. *TIGAR* knockdown markedly promoted lipid accumulation in macrophages. Silencing of *TIGAR* impaired cholesterol efflux and down-regulated the expression of ATP-binding cassette transporter A1 (ABCA1) and ABCG1 by interfering with liver X receptor  $\alpha$  (LXR $\alpha$ ) expression and activity, but did not influence cholesterol uptake by macrophages. Additionally, this inhibitory effect of TIGAR deficiency on cholesterol metabolism was mediated through the ROS/CYP27A1 pathway. *In vivo* experiments revealed that TIGAR deficiency decreased the levels of

ABCA1 and ABCG1 in plaques and aorta and impaired the capacity of RCT, thereby leading to the progression of atherosclerosis in *Apoe*<sup>-/-</sup> mice.

**Conclusions:** TIGAR mitigates the development of atherosclerosis by up-regulating ABCA1 and ABCG1 expression via the ROS/CYP27A1/LXR $\alpha$  pathway.

**KEY WORDS:** Atherosclerosis; TIGAR; ROS; CYP27A1; ABCA1; ABCG1

## 1. Introduction

Atherosclerosis (AS), a lipid-driven inflammatory disease, is the pathological basis of most cardiovascular disease including myocardial infarction and stroke <sup>[1]</sup>. Although the molecular mechanisms for atherogenesis are not fully understood, the transformation of macrophage into foam cell plays a central role in all stages of atherosclerotic lesions, from initial lesions to advanced plaques <sup>[2, 3]</sup>. This process is associated with impaired cholesterol efflux and/or uncontrolled uptake of oxidised low-density lipoprotein (ox-LDL) by scavenger receptors (SR), such as scavenger receptor-A (SR-A) and CD36 <sup>[4, 5]</sup>. Cholesterol efflux from macrophages to apolipoprotein AI (apoA-I) or high-density lipoprotein (HDL), the first and rate-limiting step of reverse cholesterol transport (RCT), is predominantly mediated by ABC transporters, including ABCA1 and ABCG1<sup>[6-9]</sup>. Therefore, a better understanding of the molecular mechanisms underlying ABCA1 and ABCG1 transporter regulation is of critical importance to develop novel therapeutic strategies for atherosclerosis.

TP53-induced glycolysis and apoptosis regulator (TIGAR), a novel p53-inducible protein, was first discovered in 2006 <sup>[10, 11]</sup>. TIGAR is now characterized as a fructose-2,6-bisphosphatase that reduces glycolysis and protects against oxidative stress <sup>[12-14]</sup>. TIGAR shares functional sequence similarities with the bis-phosphatase domain of the bifunctional enzyme PFK-2/fructose bisphosphatase-2, which reduces fructose 2,6-bisphosphate (Fru-2, 6-P<sub>2</sub>), and shifts glycolysis to the pentose phosphate pathway (PPP) to increase the reduced glutathione (GSH) and nicotinamide adenine dinucleotide phosphate (NADPH) <sup>[11]</sup>. Emerging evidence has proved that TIGAR curbs reactive oxygen species (ROS) levels and mitigates intracellular oxidative stress damage by increasing GSH and NADPH <sup>[15-17]</sup>. Furthermore, TIGAR can decrease the activities of phosphofructokinase-1 and glucose

6-phosphate dehydrogenase (G6PD), cause ATP depletion, and induce autophagy and apoptosis<sup>[18-20]</sup>. It has been reported that TIGAR is associated with heart failure<sup>[15]</sup> and myocardial infarction<sup>[21]</sup>. It is unclear, however, if TIGAR plays a role in the development of atherosclerosis. Therefore, further investigations to delineate the role and molecular mechanisms of TIGAR in atherosclerosis from the point of view of the cholesterol metabolism of macrophage foam cells are warranted.

ROS, as an essential secondary messenger, plays a crucial role in regulating cellular functions and the progression of cardiovascular diseases<sup>[22]</sup>. Relative experimental studies have shown that clearance of ROS using antioxidants is a successful and potential therapeutic strategy for preventing oxidative stress-induced pro-atherogenic events<sup>[23, 24]</sup>. 27-hydroxylase (CYP27A1), a protein located in the membrane of mitochondria, inhibits harmful buildup of cholesterol from endogenous or exogenous sources to mitochondria and converts into 27-hydroxycholesterol (27-HC), an endogenous ligand of LXR $\alpha$ . It has been reported that 27-HC is able to promote ABCA1- and ABCG1-mediated cholesterol efflux from macrophages in an LXR $\alpha$ -dependent manner<sup>[25, 26]</sup>. Recently researchers reported that loss of CYP27A1 activity is attributed to redox damage either directly to the enzyme itself or indirectly to its inner membrane surroundings in macrophages<sup>[27]</sup>. Hoshino *et al.* also demonstrated that TIGAR attenuates mitophagy and damaged mitochondria accumulation by suppressing ROS signal to prevent redox damage<sup>[21]</sup>. Therefore, it suggests that CYP27A1 may act as a bridge linking ROS to LXR $\alpha$  to involve in TIGAR-regulated lipid metabolism in the development of atherosclerosis.

In this study, the THP-1-derived macrophage and apolipoprotein E-deficient (*Apoe*<sup>-/-</sup>) mice were used to explore the roles and underlying molecular mechanisms of TIGAR on foam cell formation, RCT and atherosclerosis. We reported here the findings that *TIGAR* knockdown

increased the lipid accumulation of macrophage foam cells by decreasing ABC transporter-dependent cholesterol efflux. This detrimental effect of *TIGAR* deficiency was attributed to inhibition of the ROS/CYP27A1/LXR $\alpha$  pathway activation. The *in vivo* response to *TIGAR* deficiency may involve it in modulating hyperlipidemia and suppressing RCT, thus accelerating atherosclerosis progression. Taken together, our studies indicate the function and possible mechanism for the anti-atherogenic action of TIGAR and reveal a potential molecular target for the treatment or prevention of atherosclerosis in the future.

## 2. Materials and methods

### 2.1. Reagents

TIGAR rabbit polyclonal antibody, CD36 rabbit polyclonal antibody, SR-A rabbit polyclonal antibody, ABCA1 mouse monoclonal antibody, ABCG1 rabbit monoclonal antibody, LXR $\alpha$  rabbit monoclonal antibody, CYP27A1 rabbit monoclonal antibody,  $\beta$ -actin mouse monoclonal antibody and luciferase reporter assay kit were purchased from ABCAM (U.K.). The lentivirus-pENTR/U06-*TIGAR* shRNA and lentivirus-pENTR/U06-*CONTROL* shRNA were obtained from Invitrogen (U.S.A). The ox-LDL, dil-ox-LDL and high-density protein were purchased from Yiyuan Biotechnology (China). The apolipoprotein A-I was obtained from Sigma-Aldrich (U.S.A). Dihydroethidium (DHE) and 2',7'-dichlorofluorescein diacetate (DCFH-DA) were purchased from Beyotime (China). N-Acetyl-L-cysteine (NAC), apocynin (APO) and T0901317 were obtained MedChemExpress (U.S.A). 27-hydroxycholesterol ELISA Kit was purchased from AbeBio (China).

### 2.2 Bioinformatics analysis

The gene expression profiles of human normal arterial intima and advanced atherosclerotic plaques (GSE97210), THP-1 macrophages and THP-1 macrophage-derived foam cells (GSE54039) were obtained from Gene Expression Omnibus (GEO) datasets in the National Center for Biotechnology Information (NCBI) Database (<http://www.ncbi.nlm.nih.gov/geo/>). The differentially expressed genes were analyzed by using the limma package in R (3.6.1 version) <sup>[28]</sup>; the criteria for differentially expressed genes were a false discovery rate <0.05, as well the fold - change >2 to select the genes to be further considered in the network construction. The heatmap and volcanos of the differentially expressed genes were generated through the pheatmap package and SangerBox Software (1.0.9 version).

### 2.3 Animal studies

The male *Apoe*<sup>-/-</sup> mice (6-8 weeks of age) were purchased from Cavens lab animal (China). These mice were randomly divided into two groups with 20 mice in each group. The mice were injected via the tail-vein with lentivirus-pENTR/U06 *Control* shRNA (sh*Con*,  $5 \times 10^7$  TU/mouse) or lentivirus-pENTR/U06 *TIGAR* shRNA (sh*TIGAR*,  $5 \times 10^7$  TU/mouse). The mice were then fed a Western diet (21% fat, 0.3% cholesterol; Research Diets) for 16 weeks. At the end of the experiment, the mice were then anesthetized and euthanized for the collection of plasma, aortas, hearts and other tissues for analyses. All procedures were performed in accordance with the Institutional Animal Ethics Committee and the University of South China Animal Care Guidelines for the Use of Experimental Animals. sh*Tigar*: CACCGCGCGGAAAGGATTTCTTTGACGAATCAAAGAAATCCTTTCCGCGC; sh*Con*: CACCGGACAGTCATTGTTGAGGCTACGAATAGCCTCAACAATGACTGTC.

### 2.4 Cell culture

THP-1 monocytes were obtained from Cell Bank of the Chinese Academy of Sciences (Shanghai, China) and cultured in RPMI 1640 medium (Solarbio, China) containing 10% fetal bovine serum (FBS, Thermo, U.S.A.), 2ml L-Glutamine, 100 µg/ml streptomycin, 100 units/ml penicillin in humidified of 5% CO<sub>2</sub>, 95% air at 37°C.

### 2.5 Cell transfection

THP-1 monocytes were differentiated into macrophages by incubating with 160 nM phorbol 12-myristate 13-acetate (PMA, Sigma, U.S.A) at 24h, and cultured with fresh 10% FBS/RPMI medium for 12h. The THP-1- derived macrophages then were transfected with *TIGAR* specific shRNA or control shRNA using the lentivirus-pENTR carrier at a multiplicity of infection of 100 in the presence of 8 µg/mL polybrene. The medium was replaced with the fresh FBS/RPMI medium 12 hours after transfection. Cells were cultured for 48h

before treatment with the indicated agents. sh*TIGAR*: CATCCGCGGAAGGCAAGCCGCTAAGCCTCGAGGCTTAGCGGCTTGCCTTCCGCTTTTTG; sh*CON*: CATCCCGAAGGACGGGACATCCGACGCTCGAGCGTCGGATGTCCCGTCCTTCGTTTTTGG.

The GV219/CMC-*CYP27A1* overexpression plasmid vectors (NM\_000784) were constructed by the Genechem (Shanghai, China). The THP-1-derived macrophages were co-transfected with *CYP27A1* overexpression plasmid vectors or control vectors and sh*TIGAR* or sh*Con*, the medium was then switched to the fresh FBS/RPMI, followed by various experiments.

## 2.6 Foam cell formation evaluated by Oil Red O staining

The THP-1-derived macrophages were incubated with 50 µg/ml ox-LDL for 48h to induce foam cell formation. The cells were then washed with PBS and fixed with 4% paraformaldehyde for 10 min. After that, cells were incubated with isopropanol for 5 min, stained with 0.5% Oil Red O for 30 min, washed with 85% isopropanol, followed by staining with hematoxylin for counterstaining. Lastly, the stained cells were photographed at ×400 magnifications.

## 2.7 Lipid content assay by high-performance liquid chromatography (HPLC)

The THP-1-derived macrophages treated with 50 µg/ml ox-LDL were broken in 1 ml 0.9% NaCl using the ultrasonic processor (SONICS, USA) with 600W for 6 rounds of shaking 4s and pause 8s under ice bath. The samples were collected by centrifugation (12000g, 5min). The samples were divided into three parts. One part was measured the total protein concentrations using BCA Protein Assay Kit (Beyotime, China) for standardization. The other two parts of the sample were supplemented with isovolumetric 15% KOH, 6% trichloroacetic acid and vortex oscillation the intermixture to extract cholesterol by n-hexane- isopropanol (3:2, V/V) to measure the content of free cholesterol

and total cholesterol. Reaction mixture (500 mM MgCl<sub>2</sub> 500 mM Tris-HCl (PH=7.4), 10 mM dithiothreitol and 5% NaCl) was added into the sample or cholesterol standard calibration solution. Before measuring the total cholesterol in each sample, 0.4 U cholesterol esterase was added at 37 °C for 30 min, and then stopped by methanol: ethanol (1:1, V/V). After placed on ice for 30 min, the supernatant was collected using centrifugation with 3500 rpm for 10 min at 4 °C and then tested by 2790 Chromatographer (Waters, U.S.A). The column was eluted with isopropanol: n-heptane: acetonitrile (35:12:53) at 1 ml/min flow rate for 12 min. Absorbance at 226 nm was detected. The free cholesterol of samples was directly detected without adding cholesterol esterase. The value of cholesterol esters was estimated as the value of the total cholesterol minus free cholesterol.

### **2.8 Dil-ox-LDL uptake assay**

THP-1-derived macrophages were transfected with *TIGAR* shRNA or *CONTROL* shRNA and then treated with 10 µg/ml Dil-ox-LDL for 4h at 37 °C. Fluorescence microscopy was used to examine the fluorescence intensity of the cells and the images were acquired at identical exposure time.

### **2.9 Cholesterol efflux assay**

Cholesterol efflux assay was performed as previously described [8]. The apolipoprotein A-I was obtained from Sigma-Aldrich (U.S.A), and HDL isolated from human plasma purchased from Yiyuan Biotechnology (Guangzhou, China). Briefly, THP-1-derived macrophages were incubated with 50 µg/mL of ox-LDL and 5 µCi/mL of <sup>3</sup>H-cholesterol for 24 h. After washed three times with phosphate-buffered saline, the cells were incubated with serum-free medium for 2h at 37°C. The RPMI medium containing 20 µg/mL apoA-I or 50 µg/mL HDL (referred to our previous researches) replaced the serum-free medium and incubated at 37 °C for 12 h. The RPMI medium was then collected to measure by liquid scintillation counting. The cells were also collected and

dissolved to determine the total protein and radioactivity. The efflux capacity was expressed as the percent between  $dpm_{\text{medium}}$  and  $dpm_{\text{medium+lysate}}$ .

### 2.10 Luciferase reporter gene assay

293T cells were seeded in 6-well plates and cultured in DMEM medium (Solarbio, China) containing 10% FBS and 1% penicillin-streptomycin in a humidified atmosphere with 5% CO<sub>2</sub> at 37 °C. *Renilla* luciferase vectors with the *LXRE* region were constructed by Genechem (Shanghai, China). 293T cells were co-transfected with 0.5 µg of the *LXRE* region reporter construct and 0.5 µg of the full-length human *LXRα* expression plasmid (Genechem) using Lipofectamine 2000 (Invitrogen, U.S.A). After 12h, the cells were washed with PBS and treated with shTIGAR or shCon for 24h. The cells were lysed in a reporter lysis buffer. Luciferase activity was measured using the Dual-Glo Luciferase Assay System (Promega, U.S.A), and then normalized to the corresponding luciferase activity and plotted as a percentage of the control.

### 2.11 Quantitative polymerase chain reaction (qPCR)

Total RNAs from cells or tissues were extracted using TRIzol reagent (Beyotime, China). The cDNA was synthesized using iScript cDNA Synthesis Kit (Bio-rad, U.S.A). Then, individual quantitative RT-PCR was measured using the iCycler IQ Real-Time Detection System (BioRad, U.S.A) with gene-specific primers (Sangon Biotech, China). Primers were shown in Sup Table 1.

### 2.12 Western blotting assay

The cells and tissues were lysed with the RIPA buffer (Beyotime, China) containing 0.1 mmol/L PMSF (Beyotime, China) on ice for 30 min. The supernatants were collected by centrifugation (12000rpm, 10min, 4°C) and then measured with the BCA assay. Aliquots of the samples were subjected to SDS-PAGE, and then transported on polyvinylidene difluoride (PVDF) membranes (Millipore Corporation, U.S.A.). With blocked with 5% skim milk for

2h, the PVDF membranes were incubated with primary antibodies and respective secondary antibodies. The protein bands were visualized with BeyoECL Plus Kit (Beyotime, China) and quantified using Gel-Pro software (version 4.0).

### 2.13 Measurement of intracellular ROS levels

The pre-treated THP-1 macrophages were washed with PBS and incubated with 10  $\mu\text{mol/L}$  DHE or 10  $\mu\text{mol/L}$  DCFH-DA in the medium for 30min at 37°C. Subsequently, the medium was removed and replaced with fresh medium. Fluorescence intensity of the cells were examined by fluorescence microscopy and the images were acquired at identical exposure time. The mean fluorescence intensity (MFI) of DCF (green) and ETH (red) was measured to quantify the levels of ROS by Image Pro Plus.

### 2.14 Reverse cholesterol transport (RCT) assay

The *Apoe*<sup>-/-</sup> mice were treated with *Tigar* shRNA or *Control* shRNA and fed the Western diet. J774 macrophages were incubated with 50  $\mu\text{g/mL}$  ox-LDL and 5  $\mu\text{Ci/mL}$  [<sup>3</sup>H] cholesterol for 48h, and then suspended in DMEM. The *Apoe*<sup>-/-</sup> mice were injected intraperitoneally with the labeled J774 suspension ( $4.5 \times 10^8$  cells/mouse, n = 5/group) and then fed in the metabolic cage for 48h. The plasma samples were collected at 6, 24, and 48 h after injection to determine the radioactivity of [<sup>3</sup>H] cholesterol. The liver was isolated from euthanized mice and then extract the lipids to detect the radioactivity in the end of the experiment. Feces of individually housed mice were collected continuously for 48 h, and then freeze-dried and soaked in ethanol for scintillation counting. The data were shown as the percentage of the counts.

### 2.15 Plasma lipid profiles

The blood samples were collected into EDTA-coated tubes from the experimental mice before euthanized. The plasma was gathered using a centrifugation (3500 rpm, 4 °C, 10 min). The plasma levels of total cholesterol

(TC), high-density lipoproteins cholesterol (HDL-c) and triglycerides (TG) were measured using enzymatic methods using specific kits (Biosino, China). The value of plasma low-density-lipoproteins cholesterol (LDL-c) was estimated as the value of TC minus HDL-c and  $0.2 \times \text{TG}$ .

### **2.16 Atherosclerosis analysis**

The heart and whole aorta were immediately isolated from the ascending aorta to the ileum bifurcation after the mice were euthanized and fixed using 4% paraformaldehyde. Subsequently, the thoroughly clean aorta was split under a dissecting microscope, and then the en face of the whole aorta was staining in Oil Red O solution. After 30 min, the surface of Oil Red O-positive of the aorta was photographed with a digital camera to analyze the atherosclerotic burden of aorta. The data were showed as the percent of the positive area and the whole face area of the aorta. The heart was embedded in OCT compound (Sakura, U.S.A) and serial sectioned (8  $\mu\text{m}$  thick) throughout the three aortic valves. The eight sections of each aortic root were collected for the analysis. Oil Red O, hematoxylin and eosin (H&E) and Masson's trichrome staining were performed to evaluate the lipidoses, plaque area and plaque stability of cross-sectional. Lesion areas and percentage were quantified with Image Pro Plus software (version 6.0).

### **2.17 Statistical analysis**

Data were expressed as the means  $\pm$  SD. Statistical differences were analyzed by Student's *t*-test of two group comparisons or two-way ANOVA with *Tukey's post hoc* test of more than two group comparisons. Statistical analyses were performed using SPSS 24.0 and GraphPad Prism software (version 8.00). *p* values  $< 0.05$  ( $p < 0.05$ ) was considered statistically significant.

### 3. Results

#### 3.1 Increased *TIGAR* expression in macrophage-derived foam cells and atherosclerotic plaques

To identify differentially expressed genes in human atherosclerotic plaques, we downloaded and analyzed the GSE97210 and GSE54039 from the GEO Datasets, which the public database stores curated gene expression datasets, original series and platform records. We found that *TIGAR* expression was higher in human advanced atherosclerotic plaques than normal arterial intima, as showed in the Heatmap and volcano (Fig 1A and B). *TIGAR* expression was also increased in macrophage-derived foam cells (Fig 1C). In addition, we measured the expression of *TIGAR* in macrophage-derived foam cells by qPCR and Western blot, and the obtained data were consistent with the results of bioinformatics analyses (Fig 1D). These data suggest that *TIGAR* is related to foam cell formation and atherosclerosis progression.

#### 3.2 *TIGAR* knockdown promotes lipid accumulation in macrophages

Here we determined whether *TIGAR* affects foam cell formation. We transduced THP-1-derived macrophages with lentiviral vector expressing *TIGAR* shRNA and found that *TIGAR* was effectively silenced (Fig. 1E). Knockdown of *TIGAR* markedly increased intracellular lipid droplets in THP-1-derived macrophages treated with ox-LDL, as evidenced by Oil Red O staining (Fig 1F and G). Similarly, the HPLC analysis showed that intracellular free cholesterol (FC), total cholesterol (TC), and cholesterol ester (CE) contents were significantly increased in response to *TIGAR* knockdown (Fig 1H). In addition, we found that the intracellular triglyceride was also increased in *TIGAR* knockdown macrophages (Supplementary Fig 1). These results suggest that silencing of *TIGAR* contributes to lipid accumulation in macrophages.

### **3.3 *TIGAR* knockdown inhibits ABCA1- and ABCG1-dependent cholesterol efflux, but does not influence cholesterol uptake in macrophages.**

It is well known that cellular lipid accumulation is caused by increased cholesterol uptake and/or decreased cholesterol efflux [29]. To reveal the mechanisms by which *TIGAR* regulates lipid accumulation, THP-1-derived macrophages were treated with or without *TIGAR* shRNA. Our results showed that macrophage *TIGAR* knockdown had no effects on cholesterol uptake by measuring the Dil-ox-LDL signal in the cells (Fig 2A and B). Consistently, SR-A and CD36, two major receptors responsible for cholesterol uptake, were unchangeable in response to *TIGAR* knockdown (Fig 2C and D). In contrast, *TIGAR* knockdown significantly reduced cholesterol efflux to apoA- I and HDL (Fig 2E and F). ABCA1 and ABCG1, the ABC transporters, are the key proteins which promote cholesterol efflux to apoA-I or/and HDL [9]. As Figure 2G and H shows, ABCA1 and ABCG1 expression was down-regulated in the *TIGAR* shRNA macrophages, indicating ABCA1 and ABCG1 played an important role in the regulation of cholesterol efflux in *TIGAR* knockdown macrophages. Therefore, these results suggest that silencing of *TIGAR* inhibits ABCA1 and ABCG1 expression to reduce cholesterol efflux and promotes lipid accumulation.

### **3.4 The ROS-CYP27A1-LXR $\alpha$ pathway is involved in down-regulation of ABCA1 and ABCG1 expression induced by *TIGAR* knockdown.**

Next, we explored the underlying mechanisms by which *TIGAR* regulates ABCA1 and ABCG1 expression. As shown in Fig 3A and B, treatment of THP-1-derived macrophages with *TIGAR* shRNA markedly decreased the expression and activity of LXR $\alpha$  (Fig. 3A and B), a key transcription factor to stimulate gene transcription of *ABCA1* and *ABCG1* [30]. Importantly, pretreatment with T0901317, an LXRs agonist, restored LXR $\alpha$  activity (Fig 3C), and abrogated the effects of *TIGAR* knockdown on ABCA1 and ABCA1

expression (Fig 3D-E). In addition, ABCA1 and ABCG1 expression was unchangeable in *TIGAR* knockdown macrophages treated with LXR $\alpha$  siRNA (Supplementary Fig 2). These results indicate that silencing of *TIGAR* down-regulates both transporters expression in an LXR $\alpha$  dependent manner.

CYP27A1 can catalyze cholesterol to generate 27-hydroxycholesterol (27-HC), an endogenous ligand of LXRs<sup>[31, 32]</sup>. We speculated whether CYP27A1 is involved in *TIGAR*-mediated regulation of ABCA1 and ABCG1 expression. Indeed, *TIGAR* knockdown inhibited CYP27A1 expression and decreased 27-HC levels in THP-1-derived macrophages (Fig. 3F and G), but had no influence on the amounts of other oxysterols (Supplementary Fig 3). Importantly, the inhibitory effects of *TIGAR* knockdown on 27-HC production (Fig 3H) as well as the expression of LXR $\alpha$ , ABCA1 and ABCG1 were reversed by *CYP27A1* overexpression (Fig 3I-K), suggesting the involvement of CYP27A1 in *TIGAR* knockdown-induced down-regulation of ABCA1 and ABCG1 expression.

ROS is an essential secondary messenger and plays an important role in regulating cellular functions and the progression of cardiovascular disease<sup>[22]</sup>. Previous researches have shown that *TIGAR* can mitigate intracellular oxidative stress by decreasing ROS levels<sup>[16]</sup>, and CYP27A1 activity and 27-HC production were inhibited under the condition of oxidative stress<sup>[27]</sup>. Therefore, we inferred that ROS may be a potential mediator to connect *TIGAR* and CYP27A1. DCFH-DA and DHE were used to measure ROS levels. Our results showed that transfection with *TIGAR* shRNA dramatically promoted ROS production in THP-1-derived macrophages (Fig 4A-D). Subsequently, THP-1-derived macrophages were treated with NAC and APO to deplete ROS, followed by transduction with *TIGAR* shRNA. We found that the inhibitory effects of *TIGAR* knockdown on 27-HC production (Fig 4E and Supplementary Fig 4A), expression of CYP27A1, LXR, ABCA1 and ABCG1 (Fig 4F-I and Supplementary Fig 4B-E), cholesterol efflux (Fig 4J-K and

Supplementary Fig 4F-G) were abrogated by NAC or APO pretreatment. In addition, specific inhibitors of major signaling pathways modulated by ROS were used to measure the cholesterol efflux from macrophages. The results showed that TIGAR knockdown did not alter the efficiency of cholesterol efflux in the presence or absence of these specific inhibitors (Supplementary Fig 5). This suggests that the signaling pathways modulated by ROS is not involved in the regulation of TIGAR on macrophage cholesterol efflux. Taken together, these data demonstrate that *TIGAR* knockdown down-regulates ABCA1 and ABCG1 expression through the ROS/CYP27A1/LXR $\alpha$  pathway.

### **3.5 *Tigar* knockdown blocks RCT and accelerates the development of atherosclerosis in *Apoe*<sup>-/-</sup> mice**

Finally, to determine the role of *Tigar* in atherogenesis *in vivo*. *Apoe*<sup>-/-</sup> mice were treated with lentivirus-pENTR/U06 *Control* shRNA or *Tigar* shRNA and fed a Western diet for 16 weeks. Histological examinations revealed that the number and size of lipid-laden plaque areas in the entire *en face* aorta by Oil Red O staining of *Tigar* shRNA-treated *Apoe*<sup>-/-</sup> mice were significantly greater than those in vehicle-treated *Apoe*<sup>-/-</sup> mice (Fig 5A and B). Analysis of HE, Oil Red O and Masson's trichrome staining of cross-sections of the aortic root also showed a significant increase in the lesion area of *Apoe*<sup>-/-</sup> mice with *Tigar* knockdown (Fig 5C-F). We further characterized macrophage infiltration in the plaque using immunohistochemistry staining and found that knockdown of *Tigar* increased the amount of CD68 positive cells in the plaques (Fig 5G and H). These data suggest a protective role of *Tigar* in development of atherosclerosis. Given the critical roles of lipid metabolism disorder in the development of atherosclerosis, we detected the plasma lipid profiles in mice. Knockdown of *Tigar* significantly decreased plasma HDL-c levels, but increased plasma levels of TC and LDL-c without any effects on body weight and TG levels (Fig 5I and J). Furthermore, RCT efficiency was decreased in response to *Tigar* knockdown (Fig 5K-M). In addition, the expression of relative

proteins that play an important role in RCT was measured *in vivo*. The immunofluorescence confirmed that knockdown of *Tigar* reduced the expression of ABCA1 and ABCG1 in atherosclerotic plaques (Fig 5N-O). At the same time, decreased expression of *Tigar*, *Cyp27a1*, *Lxra*, *Abca1* and *Abcg1* was observed in the aorta from the *Apoe*<sup>-/-</sup> mice treated with *Tigar* shRNA (Fig 5P-Q). Collectively, these findings suggest *Tigar* knockdown impairs the capacity of RCT and aggravates atherosclerosis *in vivo*.

Journal Pre-proof

#### 4. Discussion

The present study has revealed the essential role of TIGAR in suppressing the formation of foam cells and the development of atherosclerosis. Our data indicated that silencing of *TIGAR* impaired ABC transporter-dependent cholesterol efflux, as well as the expression of CYP27A1 and LXR $\alpha$  following ox-LDL treatment. Moreover, *TIGAR* knockdown markedly increased ROS levels but decreased 27-HC production. Furthermore, these detrimental effects of TIGAR knockdown on ABC transporter-dependent cholesterol efflux and lipid accumulation were blunted by treatment with the ROS scavenger NAC or ROS generation inhibitor APO, CYP27A1 overexpression or LXR $\alpha$  agonist. In addition, *TIGAR* knockdown worsened deregulation of cholesterol metabolism and ultimately resulted in the progression of atherosclerosis in *Apoe*<sup>-/-</sup> mice as an *in vivo* model. Collectively, we firstly provide evidence that TIGAR is protective against atherosclerosis.

Although p53 is a well-characterized tumor suppressor, its roles in various aspects of cellular metabolism are beginning to be understood [11, 33]. Recent studies have found that p53 suppresses the mevalonate pathway and regulates ABCA1 expression [34]. TIGAR, the product of a p53 target gene, alters the pathway in which a cell uses glucose [10]. However, the role of TIGAR in lipid metabolism is still not known. Using bioinformatics analyses, we found that TIGAR expression was significantly increased in macrophage-derived foam cells, suggesting the involvement of TIGAR in the regulation of cholesterol metabolism. When the *TIGAR* was silenced, our experimental data surprisingly showed that lipid accumulation in the macrophage-derived foam cells and the progression atherosclerosis of *Apoe*<sup>-/-</sup> mice was obviously alleviated. Therefore, increased TIGAR expression in macrophage-derived foam cells and atherosclerotic plaques may result from the feedback regulatory mechanism or decompensation *in vivo* or cells. But we did not find the concrete mechanism of the TIGAR feedback or decompensation in this

research and we will focus on it in the future.

Prevention of lipid accumulation is most likely a critical mechanism by which TIGAR mitigates atherosclerosis. The macrophage foam cells formation and deposition in the intima of the aorta are a key event in the initiation and development of atherosclerosis [29]. RCT is a crucial process of transporting cholesterol from atheromatous plaques to liver for clearance, and ABCA1 and ABCG1-mediated cholesterol efflux are the key steps in this process [9]. In the previous studies, we have demonstrated that decreased expression of ABCA1 or ABCG1 in macrophages inhibits cholesterol efflux and increases cholesterol accumulation in foam cells, leading to impaired RCT and the acceleration of atherosclerosis [7-8, 35-36]. Our current findings further confirmed this notion by providing evidence that TIGAR knockdown decreased ABCA1 and ABCG1 expression and impaired cholesterol efflux, leading to a significant increase in intracellular cholesterol accumulation in macrophages following ox-LDL challenge *in vitro*. Consistently, the *ApoE*<sup>-/-</sup> mice treated with *Tigar* shRNA altered the lipoprotein cholesterol levels, impaired RCT and increased atherosclerotic plaque area *in vivo*.

ROS-elicited oxidative stress deregulates intracellular signaling cascades and cellular functions in the initial stage of cardiovascular disease [37, 38]. Accumulating evidence suggests that TIGAR induces the pentose phosphate shunt and increases NADPH generation and GSH levels to promote the removal of ROS. Clearance of ROS might be required for the beneficial effects of TIGAR on cholesterol metabolism in macrophage foam cells. Indeed, our findings suggest that knockdown of *TIGAR* decreased ABCA1 and ABCG1-mediated cholesterol efflux through ROS in macrophages, and treatment with NAC or APO abrogated the detrimental effects of *TIGAR* silencing. In addition, ROS can modulate the PI3K/AKT, Ras/MAPK and SRC/PKC signaling pathways to accelerate atherosclerosis [39]. Our results showed that blocking this signaling pathway did not affect the beneficial effect

of TIGAR on macrophage cholesterol efflux, suggesting that these signaling pathways are not implicated in the antiatherogenic action of TIGAR.

LXRs, the cholesterol-sensing nuclear receptors, play a vital role in regulating cholesterol homeostasis in macrophages and the pathogenesis of atherosclerosis [39, 40]. Previous studies have shown that LXR $\alpha$  activation ameliorates lipid accumulation by promoting ABCA1- and ABCG1-dependent cholesterol efflux in macrophage foam cells and slows down the progression of atherosclerosis [41-43]. Here, our data showed that *TIGAR* knockdown down-regulated the expression of LXR $\alpha$ , ABCA1, and ABCG1, impaired cholesterol efflux, and promoted the progression of atherosclerosis. In addition, LXR $\beta$  expression was decreased in the *TIGAR* knockdown macrophages (Supplementary Fig 6). This suggests that LXRs may be the important transcription factors to participate in the TIGAR-inducing ABCA1 and ABCG1 expression. Moreover, activation of ROS by TIGAR knockdown inhibited LXRs-induced up-regulation of ABCA1 and ABCG1 expression in macrophages. The observations are consistent with a previous study showing that the beneficial effects of LXRs on cholesterol efflux are repressed by triggering NOX-ROS signaling [44]. In addition, autophagy can contribute to cholesterol efflux by degradation of lipid drops [45] and TIGAR also can regulate autophagy by ROS [46]. Autophagy may be also involved in the beneficial effect of TIGAR on macrophage cholesterol efflux, but it is necessary to clarify this possibility in further studies.

Our current findings further explained the underlying mechanism of ROS on LXR $\alpha$  inactivation, to which CYP27A1 may be a mediator. Consistently, our current findings showed that overexpression of CYP27A1 abrogated TIGAR-mediated LXR $\alpha$ , ABCA1 and ABCG1 expression and treatment with NAC or APO blocked TIGAR deficiency-induced deregulation of CYP27A1 in macrophages. It was reported that CYP27A1 activity and 27-HC production were inhibited by oxidative stress [27]. Thus, we think that increased ROS by

silencing *TIGAR* may be the major reason to inhibit CYP27A1 expression and activity, and 27-HC production. However, we do not have direct evidence to support the effect of ROS on CYP27A1 and the underlying mechanism. Thus, additional studies to delineate the effect of TIGAR-ROS signaling on CYP27A1-LXR $\alpha$ -ABC transporters mediated cardiovascular benefits are warranted.

However, there are several limitations in our study. Firstly, our *in vitro* experiments employed the human THP-1 cell line without primary human monocyte-derived macrophages to confirm the implication of TIGAR in cholesterol metabolism in macrophages. Secondly, we did not establish specific-macrophage knockout *Tigar* animal models to explore the implications of macrophage-specific *Tigar* on atherosclerosis development. Thirdly, the implications of TIGAR on the liver were not investigated in this study. Fourthly, we only focused on the role of lipid transporters and not on other pathways. For instance, autophagy may also participate in the beneficial effect of TIGAR on macrophage cholesterol efflux and atherosclerosis.

In summary, we provide the first evidence for the beneficial effects of TIGAR on atherosclerosis. Mechanistically, TIGAR decreases the levels of ROS and activates the CYP27A1/LXR $\alpha$  pathway, which up-regulates ABCA1 and ABCG1 expression and promotes cholesterol efflux (Fig 6). Therefore, findings from our study shed light on the mechanisms by which TIGAR restrains the development of atherosclerosis and indicate that targeting TIGAR may be a potential approach to prevent and treat atherosclerotic cardiovascular disease.

## 5. Declaration of competing interests

The authors declare that they have no known competing financial interests or personal relationships that could have appeared to influence the work reported in this paper.

## 6. Author contributions

Zhen-Wang Zhao, Min Zhang, Jin Zou, Conception, design, execution of the experiments, analysis and interpretation of data and writing of the initial draft of the manuscript. Xiang-Jun Wan, Li Zhou, Yao Wu, worked with the *Apoe*<sup>-/-</sup> model of atherosclerosis. Shang-Ming Liu, Ling-Xiao Liao, Heng Li, Yu-Sheng Qin, worked with the cell experiment. Xiao-Hua Yu, Chao-Ke Tang, critically evaluated and edited the manuscript.

## 7. Acknowledgments

The authors gratefully acknowledge the financial support from the National Natural Sciences Foundation of China (81770461).

## 8. References

1. J. Boren, M.J. Chapman, R.M. Krauss, C.J. Packard, J.F. Bentzon, C.J. Binder, M.J. Daemen, L.L. Demer, R.A. Hegele, S.J. Nicholls, B.G. Nordestgaard, G.F. Watts, E. Bruckert, S. Fazio, B.A. Ference, I. Graham, J.D. Horton, U. Landmesser, U. Laufs, L. Masana, G. Pasterkamp, F.J. Raal, K.K. Ray, H. Schunkert, M.R. Taskinen, B. van de Sluis, O. Wiklund, L. Tokgozoglu, A.L. Catapano, H.N. Ginsberg, Low-density lipoproteins cause atherosclerotic cardiovascular disease: pathophysiological, genetic, and therapeutic insights: a consensus statement from the European Atherosclerosis Society Consensus Panel, *Eur Heart J* 41 (24) (2020) 2313-2330.
2. Y. Liu, Y. Zhong, H. Chen, D. Wang, M. Wang, J.S. Ou, M. Xia, Retinol-Binding Protein-Dependent Cholesterol Uptake Regulates Macrophage Foam Cell Formation and Promotes Atherosclerosis, *Circulation* 135 (14) (2017) 1339-1354.
3. D.A. Chistiakov, A.A. Melnichenko, V.A. Myasoedova, A.V. Grechko, A.N. Orekhov, Mechanisms of foam cell formation in atherosclerosis, *J Mol Med (Berl)* 95 (11) (2017) 1153-1165.
4. T. Kuznetsova, K.H.M. Prange, C.K. Glass, M.P.J. de Winther, Transcriptional and epigenetic regulation of macrophages in atherosclerosis, *Nat Rev Cardiol* 17 (4) (2020) 216-228.
5. J. Luo, H. Yang, B.L. Song, Mechanisms and regulation of cholesterol homeostasis, *Nat Rev Mol Cell Biol* 21 (4) (2020) 225-245.
6. X. Ou, J.H. Gao, L.H. He, X.H. Yu, G. Wang, J. Zou, Z.W. Zhao, D.W. Zhang, Z.J. Zhou, C.K. Tang, Angiotensin-1 aggravates atherosclerosis by inhibiting cholesterol efflux and promoting inflammatory response, *Biochim Biophys Acta Mol Cell Biol Lipids* 1865 (2) (2020) 158535.
7. G. Wang, J.H. Gao, L.H. He, X.H. Yu, Z.W. Zhao, J. Zou, F.J. Wen, L.

- Zhou, X.J. Wan, C.K. Tang, Fargesin alleviates atherosclerosis by promoting reverse cholesterol transport and reducing inflammatory response, *Biochim Biophys Acta Mol Cell Biol Lipids* 1865 (5) (2020) 158633.
8. Z.W. Zhao, M. Zhang, L.Y. Chen, D. Gong, X.D. Xia, X.H. Yu, S.Q. Wang, X. Ou, X.Y. Dai, X.L. Zheng, D.W. Zhang, C.K. Tang, Heat shock protein 70 accelerates atherosclerosis by downregulating the expression of ABCA1 and ABCG1 through the JNK/Elk-1 pathway, *Biochim Biophys Acta Mol Cell Biol Lipids* 1863 (8) (2018) 806-822.
  9. X.H. Yu, D.W. Zhang, X.L. Zheng, C.K. Tang, Cholesterol transport system: An integrated cholesterol transport model involved in atherosclerosis, *Prog Lipid Res* 73 (2019) 65-91.
  10. K. Bensaad, A. Tsuruta, M.A. Selak, M.N. Vidal, K. Nakano, R. Bartrons, E. Gottlieb, K.H. Vousden, TIGAR, a p53-inducible regulator of glycolysis and apoptosis, *Cell* 126 (1) (2006) 107-120.
  11. D.R. Green, J.E. Chipuk, p53 and metabolism: Inside the TIGAR, *Cell* 126 (1) (2006) 30-32.
  12. L. Yin, T. Kufe, D. Avigan, D. Kufe, Targeting MUC1-C is synergistic with bortezomib in downregulating TIGAR and inducing ROS-mediated myeloma cell death, *Blood* 123 (19) (2014) 2997-3006.
  13. H. Wang, Q. Cheng, X. Li, F. Hu, L. Han, H. Zhang, L. Li, J. Ge, X. Ying, X. Guo, Q. Wang, Loss of TIGAR Induces Oxidative Stress and Meiotic Defects in Oocytes from Obese Mice, *Mol Cell Proteomics* 17 (7) (2018) 1354-1364.
  14. S. Wang, Z. Peng, S. Wang, L. Yang, Y. Chen, X. Kong, S. Song, P. Pei, C. Tian, H. Yan, P. Ding, W. Hu, C.H. Liu, X. Zhang, F. He, L. Zhang, KRAB-type zinc-finger proteins PITA and PISA specifically regulate p53-dependent glycolysis and mitochondrial respiration, *Cell Res* 28 (5) (2018) 572-592.

15. Y. Okawa, A. Hoshino, M. Ariyoshi, S. Kaimoto, S. Tateishi, K. Ono, M. Uchihashi, E. Iwai-Kanai, S. Matoba, Ablation of cardiac TIGAR preserves myocardial energetics and cardiac function in the pressure overload heart failure model, *Am J Physiol Heart Circ Physiol* 316 (6) (2019) H1366-H1377.
16. J. Geng, M. Wei, X. Yuan, Z. Liu, X. Wang, D. Zhang, L. Luo, J. Wu, W. Guo, Z.H. Qin, TIGAR regulates mitochondrial functions through SIRT1-PGC1 $\alpha$  pathway and translocation of TIGAR into mitochondria in skeletal muscle, *Faseb j* 33 (5) (2019) 6082-6098.
17. Z.Q. Liu, N. Liu, S.S. Huang, M.M. Lin, S. Qin, J.C. Wu, Z.Q. Liang, Z.H. Qin, Y. Wang, NADPH protects against kainic acid-induced excitotoxicity via autophagy-lysosome pathway in rat striatum and primary cortical neurons, *Toxicology* 435 (2020) 152408.
18. D.M. Zhang, T. Zhang, M.M. Wang, X.X. Wang, Y.Y. Qin, J. Wu, R. Han, R. Sheng, Y. Wang, Z. Chen, F. Han, Y. Ding, M. Li, Z.H. Qin, TIGAR alleviates ischemia/reperfusion-induced autophagy and ischemic brain injury, *Free Radic Biol Med* 137 (2019) 13-23.
19. W. Zhou, Y. Yao, J. Li, D. Wu, M. Zhao, Z. Yan, A. Pang, L. Kong, TIGAR Attenuates High Glucose-Induced Neuronal Apoptosis via an Autophagy Pathway, *Front Mol Neurosci* 12 (2019) 193.
20. Z. Li, Z. Shao, S. Chen, D. Huang, Y. Peng, S. Chen, K. Ma, TIGAR impedes compression-induced intervertebral disc degeneration by suppressing nucleus pulposus cell apoptosis and autophagy, *J Cell Physiol* 235 (2) (2020) 1780-1794.
21. A. Hoshino, S. Matoba, E. Iwai-Kanai, H. Nakamura, M. Kimata, M. Nakaoka, M. Katamura, Y. Okawa, M. Ariyoshi, Y. Mita, K. Ikeda, T. Ueyama, M. Okigaki, H. Matsubara, p53-TIGAR axis attenuates mitophagy to exacerbate cardiac damage after ischemia, *J Mol Cell Cardiol* 52 (1) (2012) 175-184.

22. N. Panth, K.R. Paudel, K. Parajuli, Reactive Oxygen Species: A Key Hallmark of Cardiovascular Disease, *Adv Med* 2016 (2016) 9152732.
23. Y. Wang, L. Li, W. Zhao, Y. Dou, H. An, H. Tao, X. Xu, Y. Jia, S. Lu, J. Zhang, H. Hu, Targeted Therapy of Atherosclerosis by a Broad-Spectrum Reactive Oxygen Species Scavenging Nanoparticle with Intrinsic Anti-inflammatory Activity, *ACS Nano* 12 (9) (2018) 8943-8960.
24. A. Guides, H.R. Griffiths, A. David, G.Y. Lip, E. Shantsila, Monocytes in coronary artery disease and atherosclerosis: where are we now?, *J Am Coll Cardiol* 62 (17) (2013) 1541-1551.
25. M. Umetani, P. Ghosh, T. Ishikawa, J. Umetani, M. Ahmed, C. Mineo, P.W. Shaul, The cholesterol metabolite 27-hydroxycholesterol promotes atherosclerosis via proinflammatory processes mediated by estrogen receptor alpha, *Cell Metab* 20 (1) (2014) 172-182.
26. X. Fu, J.G. Menke, Y. Chen, G. Zhou, K.L. MacNaul, S.D. Wright, C.P. Sparrow, E.G. Lund, 27-hydroxycholesterol is an endogenous ligand for liver X receptor in cholesterol-loaded cells, *J Biol Chem* 276 (42) (2001) 38378-38387.
27. W. Korytowski, K. Wawak, P. Pabisz, J.C. Schmitt, A.C. Chadwick, D. Sahoo, A.W. Girotti, Impairment of Macrophage Cholesterol Efflux by Cholesterol Hydroperoxide Trafficking: Implications for Atherogenesis Under Oxidative Stress, *Arterioscler Thromb Vasc Biol* 35 (10) (2015) 2104-2113.
28. M.E. Ritchie, B. Phipson, D. Wu, Y. Hu, C.W. Law, W. Shi, G.K. Smyth, limma powers differential expression analyses for RNA-sequencing and microarray studies, *Nucleic Acids Res* 43 (7) (2015) e47.
29. X.H. Yu, Y.C. Fu, D.W. Zhang, K. Yin, C.K. Tang, Foam cells in atherosclerosis, *Clin Chim Acta* 424 (2013) 245-252.
30. H. Wang, Y. Yang, X. Sun, F. Tian, S. Guo, W. Wang, Z. Tian, H. Jin, Z. Zhang, Y. Tian, Sonodynamic therapy-induced foam cells apoptosis

- activates the phagocytic PPARgamma-LXRalpha-ABCA1/ABCG1 pathway and promotes cholesterol efflux in advanced plaque, *Theranostics* 8 (18) (2018) 4969-4984.
31. L.C. Mangum, X. Hou, A. Borazjani, J.H. Lee, M.K. Ross, J.A. Crow, Silencing carboxylesterase 1 in human THP-1 macrophages perturbs genes regulated by PPARgamma/RXR and RAR/RXR: down-regulation of CYP27A1-LXRalpha signaling, *Biochem J* 475 (3) (2018) 621-642.
  32. A. Graham, Mitochondrial regulation of macrophage cholesterol homeostasis, *Free Radic Biol Med* 89 (2015) 982-992.
  33. K.H. Vousden, D.P. Lane, p53 in health and disease, *Nat Rev Mol Cell Biol* 8 (4) (2007) 275-283.
  34. S.H. Moon, C.H. Huang, S.L. Houlihan, K. Regunath, W.A. Freed-Pastor, J.P.t. Morris, D.F. Tschaharganeh, E.R. Kasthuber, A.M. Barsotti, R. Culp-Hill, W. Xue, Y.J. Ho, T. Baslan, X. Li, A. Mayle, E. de Stanchina, L. Zender, D.R. Tong, A. D'Alessandro, S.W. Lowe, C. Prives, p53 Represses the Mevalonate Pathway to Mediate Tumor Suppression, *Cell* 176 (3) (2019) 564-580 e519.
  35. A.E. Bortnick, G.H. Rothblat, G. Stoudt, K.L. Hoppe, L.J. Royer, J. McNeish, O.L. Francone, The correlation of ATP-binding cassette 1 mRNA levels with cholesterol efflux from various cell lines, *J Biol Chem* 275 (37) (2000) 28634-28640.
  36. J. Klucken, C. Büchler, E. Orsó, W.E. Kaminski, M. Porsch-Ozcürümez, G. Liebisch, M. Kapinsky, W. Diederich, W. Drobnik, M. Dean, R. Allikmets, G. Schmitz, ABCG1 (ABC8), the human homolog of the *Drosophila* white gene, is a regulator of macrophage cholesterol and phospholipid transport, *Proc Natl Acad Sci U S A* 97 (2) (2000) 817-822.
  37. Y. Zhang, P. Murugesan, K. Huang, H. Cai, NADPH oxidases and oxidase crosstalk in cardiovascular diseases: novel therapeutic targets, *Nat Rev Cardiol* 17 (3) (2020) 170-194.

38. C.D. Ochoa, R.F. Wu, L.S. Terada, ROS signaling and ER stress in cardiovascular disease, *Mol Aspects Med* 63 (2018) 18-29.
39. J. Zhang, X. Wang, V. Vikash, Q. Ye, D. Wu, Y. Liu, W. Dong, ROS and ROS-Mediated Cellular Signaling, *Oxid Med Cell Longev* 2016 (2016) 4350965.
40. J. Hsieh, M. Koseki, M.M. Molusky, E. Yakushiji, I. Ichi, M. Westerterp, J. Iqbal, R.B. Chan, S. Abramowicz, L. Tascau, S. Takiguchi, S. Yamashita, C.L. Welch, G. Di Paolo, M.M. Hussain, J.H. Lefkowitz, D.J. Rader, A.R. Tall, TTC39B deficiency stabilizes LXR reducing both atherosclerosis and steatohepatitis, *Nature* 535 (7611) (2016) 303-307.
41. S. Guo, L. Li, H. Yin, Cholesterol Homeostasis and Liver X Receptor (LXR) in Atherosclerosis, *Cardiovasc Hematol Disord Drug Targets* 18 (1) (2018) 27-33.
42. P. Jin, Y. Bian, K. Wang, G. Cong, R. Yan, Y. Sha, X. Ma, J. Zhou, Z. Yuan, S. Jia, Homocysteine accelerates atherosclerosis via inhibiting LXRalpha-mediated ABCA1/ABCG1-dependent cholesterol efflux from macrophages, *Life Sci* 214 (2018) 41-50.
43. M. Vinod, I. Chennamsetty, S. Colin, L. Belloy, F. De Paoli, H. Schaidler, W.F. Graier, S. Frank, D. Kratky, B. Staels, G. Chinetti-Gbaguidi, G.M. Kostner, miR-206 controls LXRalpha expression and promotes LXR-mediated cholesterol efflux in macrophages, *Biochim Biophys Acta* 1841 (6) (2014) 827-835.
44. S.L. Tang, W.J. Chen, K. Yin, G.J. Zhao, Z.C. Mo, Y.C. Lv, X.P. Ouyang, X.H. Yu, H.J. Kuang, Z.S. Jiang, Y.C. Fu, C.K. Tang, PAPP-A negatively regulates ABCA1, ABCG1 and SR-B1 expression by inhibiting LXRalpha through the IGF-I-mediated signaling pathway, *Atherosclerosis* 222 (2) (2012) 344-354.
45. C.H. Chen, J.F. Zhao, C.P. Hsu, Y.R. Kou, T.M. Lu, T.S. Lee, The detrimental effect of asymmetric dimethylarginine on cholesterol efflux of

macrophage foam cells: Role of the NOX/ROS signaling, *Free Radic Biol Med* 143 (2019) 354-365.

46. M. Ouimet, V. Franklin, E. Mak, X. Liao, I. Tabas, Y.L. Marcel, Autophagy regulates cholesterol efflux from macrophage foam cells via lysosomal acid lipase, *Cell Metab* 13 (6) (2011) 655-667.
47. W. Hu, S. Chen, R.F. Thorne, M. Wu, TP53, TP53 Target Genes (DRAM, TIGAR), and Autophagy, *Adv Exp Med Biol* 1206 (2019) 127-149.

Journal Pre-proof

## Figure Legend.

**Fig 1.** TIGAR is involved in the formation of macrophage foam cells and atherosclerosis.

(A-C). The expression of TIGAR in atherosclerotic plaques (GSE97210) and macrophage-derived foam cells (GSE54039) was measured based on the microarray analysis (red is high expression, black is the middle and green mean low expression) and volcano plot (red is up and green is down) from GEO datasets. (D). The qPCR and Western blot analysis of *TIGAR* levels in THP-1 macrophages -derived foam cells. (E). The THP-1-derived macrophages were treated with *TIGAR* shRNA and then incubated with ox-LDL (50 µg/mL) for 24 h and the Western blot analysis of TIGAR levels in cells was performed. (F-G). The lipid accumulation of macrophages was analyzed by Oil red O staining (40×) and the Oil Red O–staining area was measured by Image Pro Plus. (H). The lipid content of macrophages-derived foam cells was measured by HPLC. Data represent mean ± SD of three experiments performed independently under the same conditions. \*  $p < 0.05$ , \*\*  $p < 0.01$  vs. shCon.

**Fig 2.** TIGAR knockdown decreases ABC transporter-dependent cholesterol efflux.

(A and B). The THP-1-derived macrophages were treated as indicated and then with 10 µg/ml Dil-ox-LDL for 4h at 37 °C. The fluorescence microscopy was used to examine the fluorescence intensity of the cells. Scale bar = 20 µm. (C-D). The qPCR and Western blot were used to measure the expression of SR-A and CD36 in macrophages. (E-F). THP-1-derived macrophages treated as indicated were incubated with ox-LDL and <sup>3</sup>H-cholesterol, and then the cells were incubated with apoA-I (E) or HDL (F). Radioactivity in culture medium and cells were measured separately using liquid scintillation counting. Cholesterol efflux to apoA-I or HDL was calculated as the percentage of [<sup>3</sup>H] cholesterol in the medium to the total in the medium and cells. (G and H). The ABCA1 and ABCG1 expression was detected in THP-1-derived macrophages by qPCR and Western blot. Data represent mean ± SD of three experiments performed independently under the same conditions. \*\*  $p < 0.01$  vs. shCon.

**Fig 3.** TIGAR knockdown reduces ABCA1 and ABCG1 expression by the CYP27A1/27-HC/LXR $\alpha$  pathway.

(A) THP-1-derived macrophages were treated with the indicated treatments and then the qPCR and Western blot were used to assess mRNA and protein levels of LXR $\alpha$ . (B and C). 293T cells were co-transfected with the plasmid encoding full-length human LXR $\alpha$  and the *Renilla* luciferase vectors with the LXRE region, and then treated with shTIGAR or shCON. The Dual-Glo Luciferase Assay System detected the luciferase activity of the cell lysis. (D and E). THP-1-derived macrophages were treated with TIGAR shRNA or CONTROL shRNA and incubated with LXR $\alpha$  agonist (T0901317, 100 nM) for 24h to detect ABCA1 and ABCG1 expression through qPCR and Western blot. (F and G). The THP-1-derived macrophages were pre-treated and then the mRNA and protein levels of CYP27A1 were detected by qPCR and Western blot analysis. (H) The levels of 27-HC were measured using ELISA. (I-K). The THP-1-derived macrophages were co-transfected with TIGAR shRNA and CYP27A1 to detect LXR $\alpha$ , ABCA1 and ABCG1 expression using qPCR and Western blot. Data represent mean  $\pm$  SD of three experiments performed independently under the same conditions. \*  $p < 0.05$ , \*\*  $p < 0.01$  vs. shCON; ##  $p < 0.01$  vs. shTIGAR.

**Fig 4.** TIGAR knockdown decreases ABC transporter-dependent cholesterol efflux by the ROS-CYP27A1/27-HC-LXR $\alpha$  pathway.

The THP-1-derived macrophages were treated as indicated. (A) The intensity of green fluorescent DCF was analyzed to assess ROS. Representative fluorescent microscopy images of ROS. Scale bar = 20  $\mu\text{m}$ . (B) The intensity of red fluorescent DHE were analyzed to detect the ROS levels. Scale bar = 150  $\mu\text{m}$ . (C-D) The mean fluorescence intensity (MFI) of DCF (green) and ETH (red) were measured by Image Pro Plus. The THP-1-derived macrophages were treated with *TIGAR* shRNA or *CONTROL* shRNA and incubated with ROS scavenger (NAC, 10 nM) for 6h. (E) The 27-HC levels were measured using ELISA. (F-I) qPCR and Western blot were performed to detect the expression of CYP27A1, LXR $\alpha$ , ABCA1 and ABCG1. (J and K) The cholesterol efflux to apoA-I or HDL was measured by liquid scintillation counter. Data represent mean  $\pm$  SD of three experiments that were performed independently under the same conditions. \*\*  $p < 0.01$  vs. shCON; ##  $p < 0.01$  vs. sh*TIGAR*.

**Fig 5.** *Tigar* knockdown decreases the capacity for RCT and increases atherosclerotic area in *Apoe*<sup>-/-</sup> mice.

Male *apoE*<sup>-/-</sup> mice were injected via the tail vein with *Control* shRNA (*shCon*), or *Tigar* shRNA (*shTigar*), and fed a Western diet for 16 weeks (20 mice per group). (A and B). The whole aortas were stained with Oil Red O (A) and the atherosclerotic burden was quantified by measuring the surface area of Oil Red O–positive lesions on *en face* preparations (B). (n = 6 mice/group). (C-F). The sixth section of serial sections (8 μm thick) of the three aortic valves from each mouse was stained with H&E, Oil Red O, or Masson. Lesion areas (D), Oil Red O-staining areas (E) and collagen content (F) were quantified with Image Pro Plus software (n = 9-10 mice/group). Scale bar = 300 μm. (G and H). Immunohistochemistry of the section of the aortic valves was labeled with the macrophage marker Cd68 and the average optical density of Cd68 staining was measured by Image Pro Plus software (n = 5 mice/group). (I) Enzymatic methods measured the levels of plasma lipids (mmol/L) including total cholesterol (TC), triglyceride (TG), high-density lipoprotein cholesterol (HDL-C) and low-density lipoprotein cholesterol (LDL-C) from *apoE*<sup>-/-</sup> mice with different treatments (n = 10 mice/group). (J) Body weight gain of the mice throughout the process (n = 20 mice/group). (K-M) [<sup>3</sup>H]-cholesterol and ox-LDL-loaded J774 macrophages were injected into *apoE*<sup>-/-</sup> mice (n = 5 mice/group). The amounts of [<sup>3</sup>H]-tracer in plasma (K), liver (L) and feces (M) were determined by scintillation counting. (N and O) Immunofluorescence staining of *Abca1* and *Abcg1* in atherosclerotic plaques. Scale bar = 80 μm. (P and Q). Total RNAs were isolated from the aorta and then subjected to qPCR to quantify mRNA levels of *Abca1* and *Abcg1*. The same amount of lysate isolated from aorta homogenate was subjected to Western blot to detect *Abca1* and *Abcg1* (n = 3 mice/group). Data represent mean ± SD, \* *p* < 0.05, \*\* *p* < 0.01 vs. *shCon*.

**Fig 6.** Schematic illustration of the proposed mechanism underlying that TIGAR promotes cholesterol efflux and mitigates the development of atherosclerosis in macrophages.

As shown, TIGAR reduces ROS production, which in turn promotes CYP27A1 activity and 27-HC production, increases LXRs activity and upregulates the expression of ABCA1 and ABCG1, leading to the facilitation of cholesterol efflux and decreasing lipid accumulation in macrophage, ultimately, acceleration RCT and mitigating the development of atherosclerosis.

Journal Pre-proof

Journal Pre-proof

Fig 1

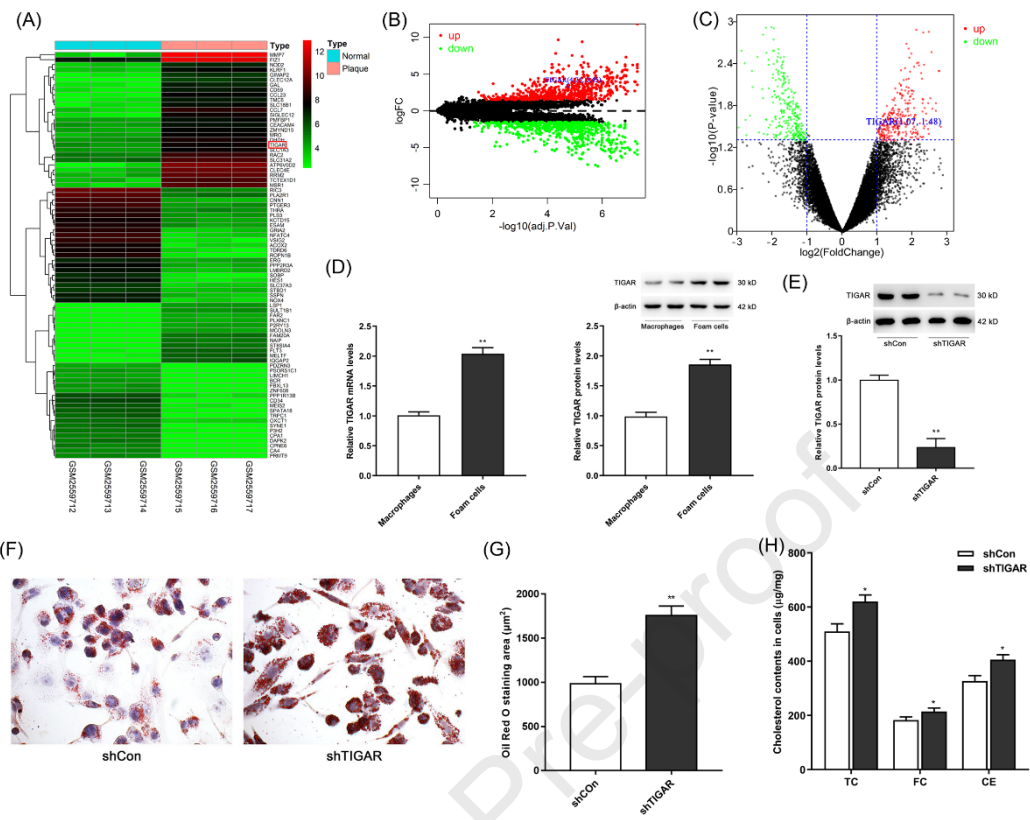


Fig 2

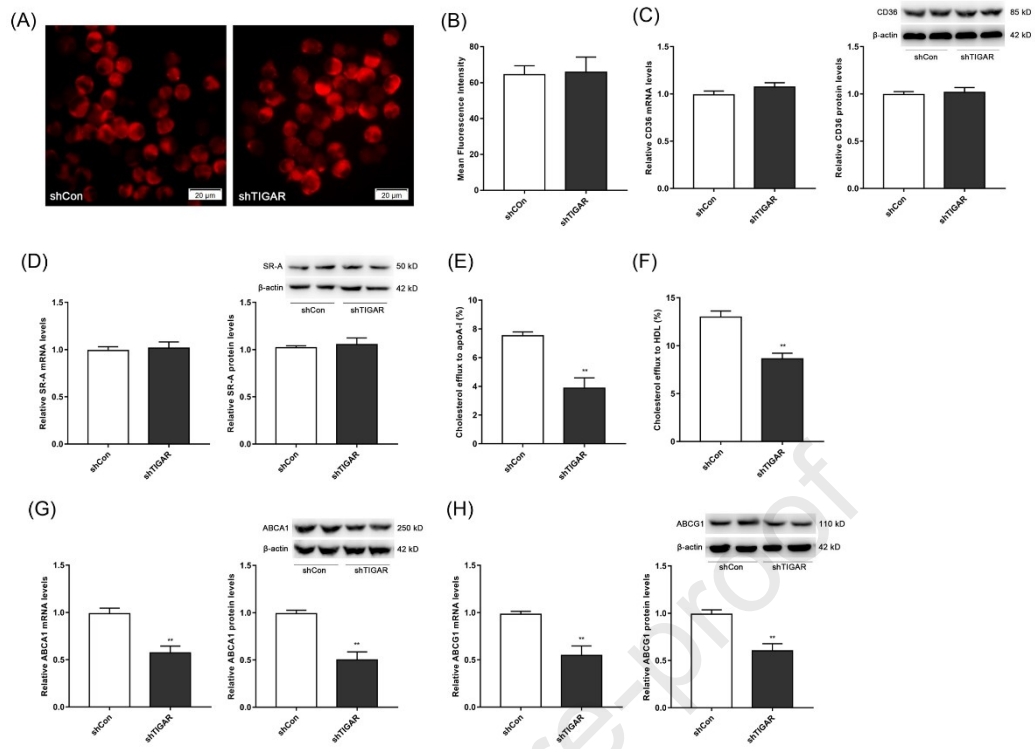


Fig 3

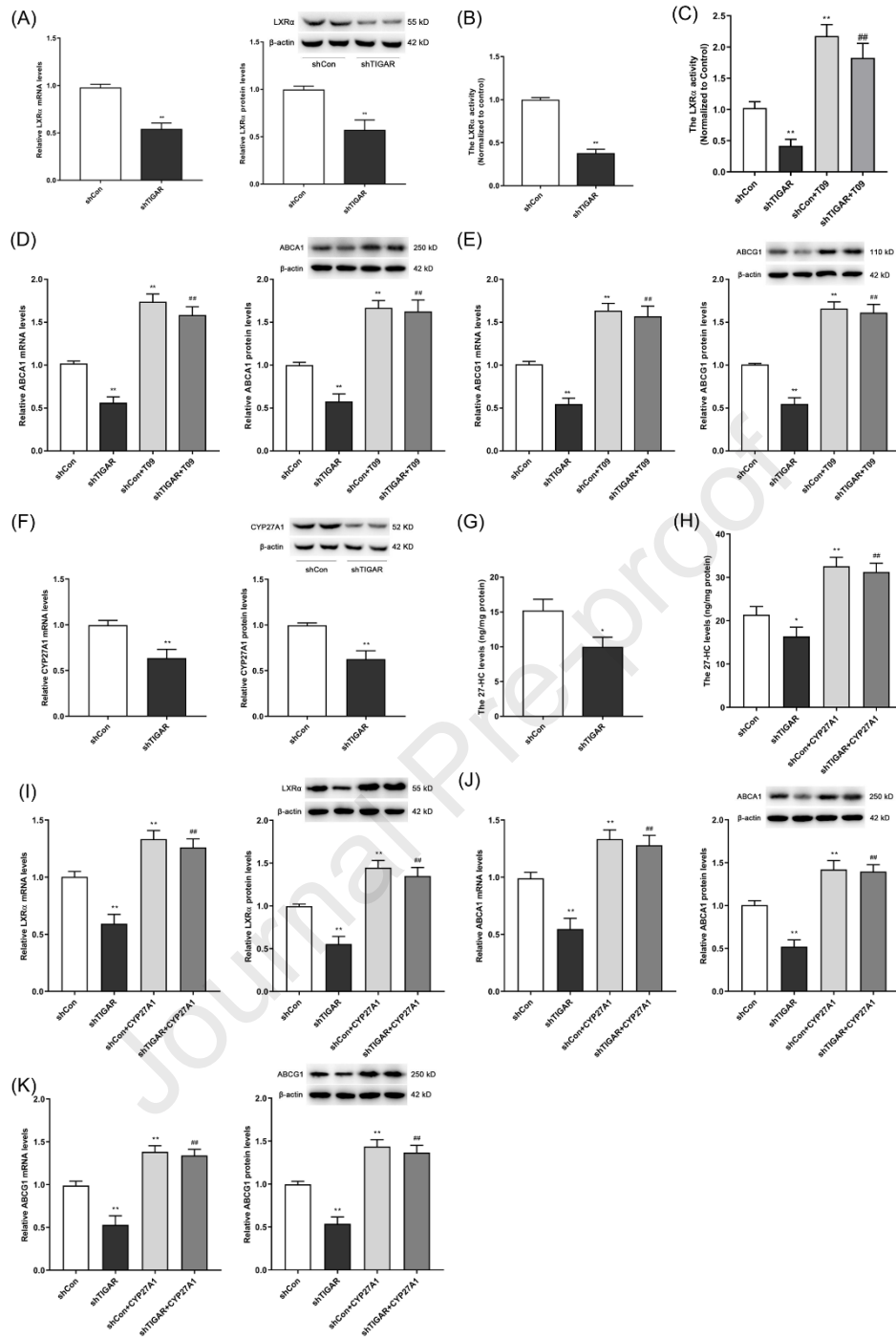


Fig 4

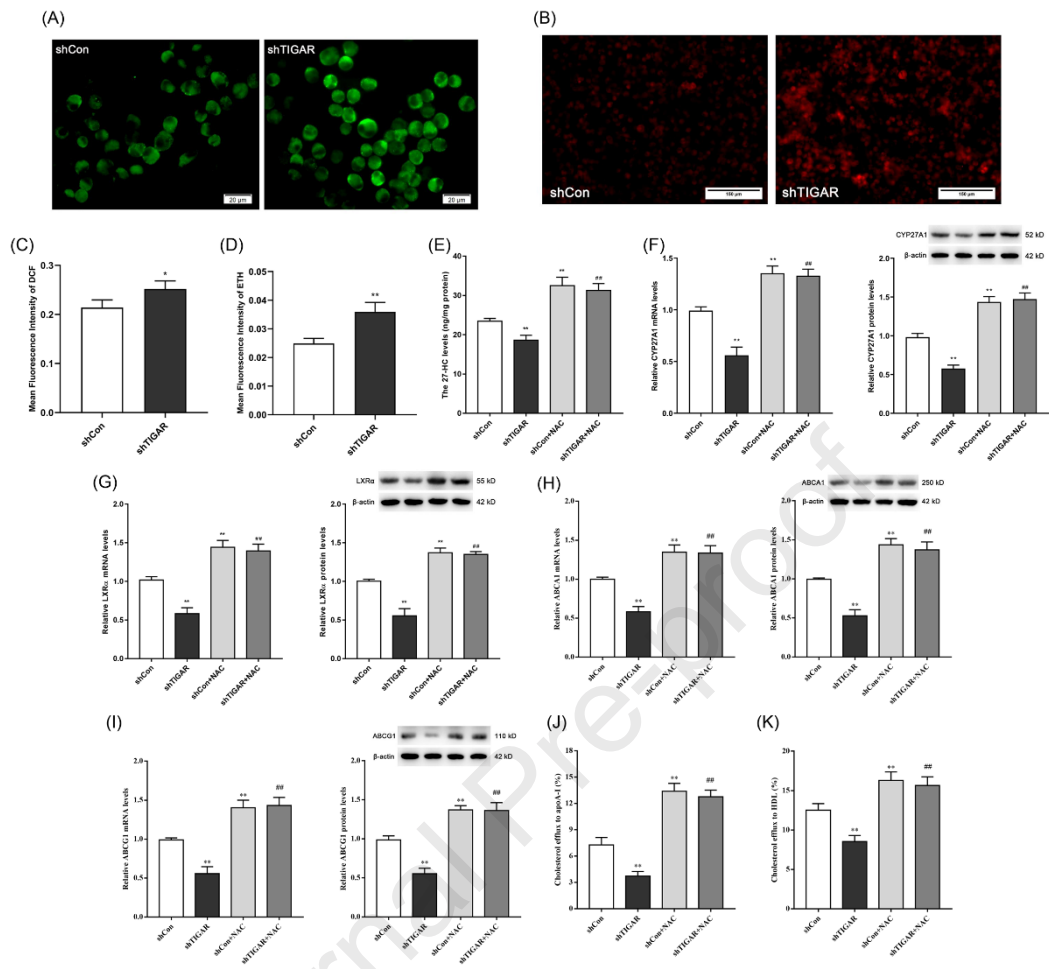


Fig 5

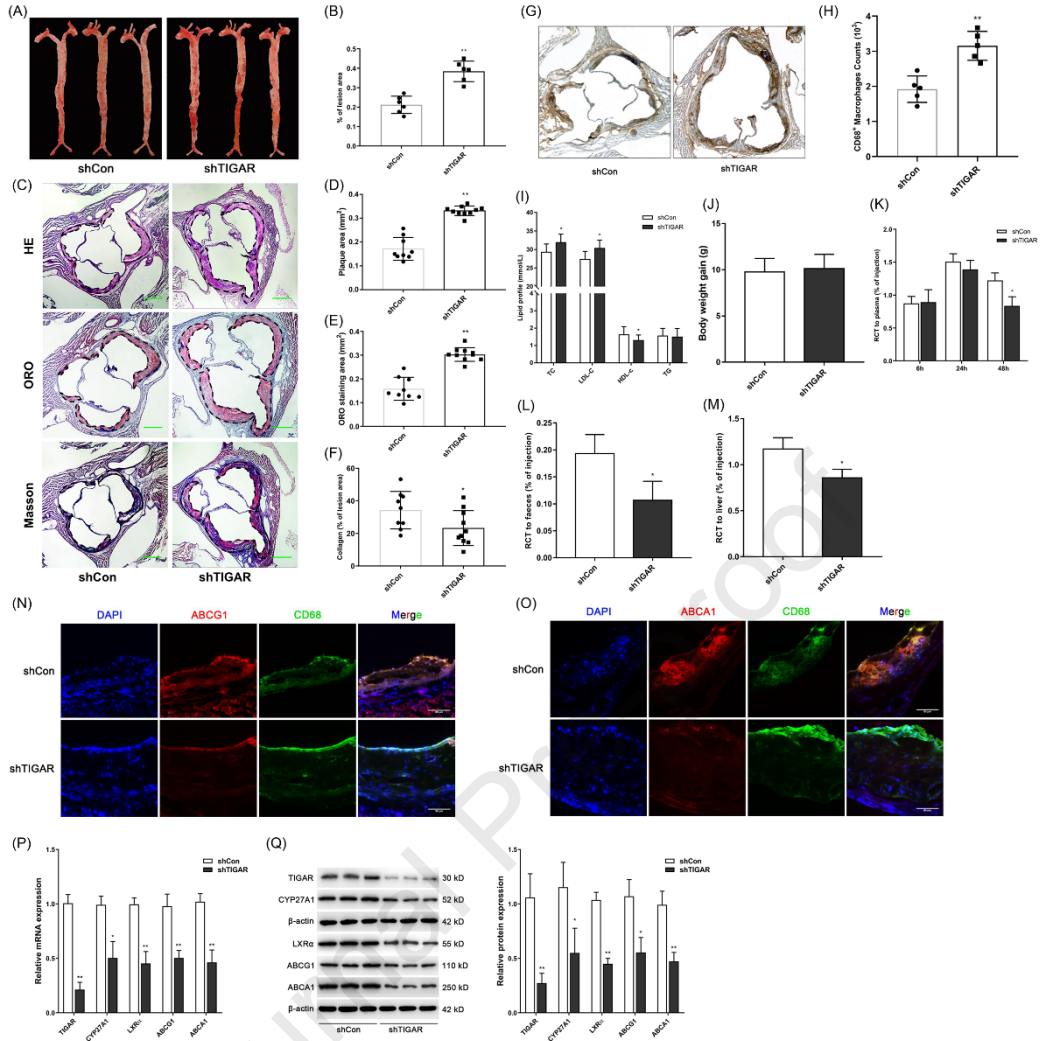
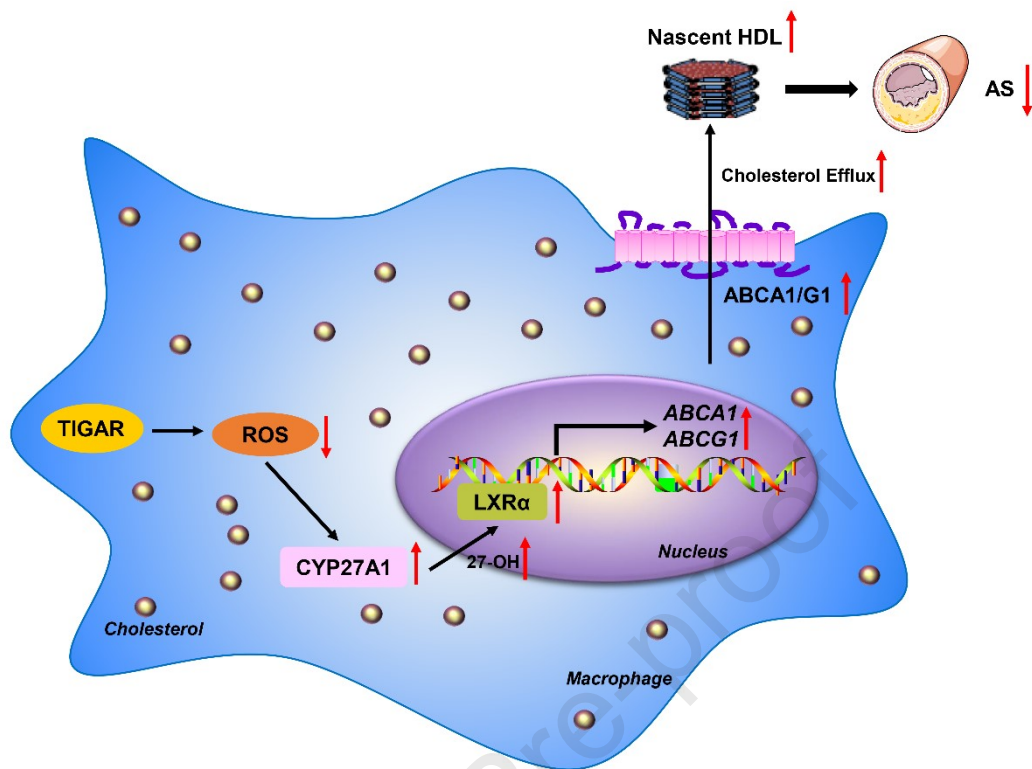


Fig 6



## Highlights

1. TIGAR is involved in the macrophage foam cells formation and atherosclerosis development.
2. TIGAR promotes ABCA1- and ABCG1-dependent cholesterol efflux, but does not influence cholesterol uptake in macrophages.
3. TIGAR increases ABCA1 and ABCG1 expression by reducing ROS and activating CYP27A1/LXR $\alpha$  pathway.
4. TIGAR facilitates RCT and mitigates the development of atherosclerosis in *Apoe*<sup>-/-</sup> mice.

### Conflict of Interests

We wish to confirm that there are no known conflicts of interest associated with this publication and there has been no significant financial support for this work that could have influenced its outcome.

We confirm that the manuscript has been read and approved by all named authors and that there are no other persons who satisfied the criteria for authorship but are not listed. We further confirm that the order of authors listed in the manuscript has been approved by all of us.

We confirm that we have given due consideration to the protection of intellectual property associated with this work and that there is no impediment to publication, including the timing of publication, with respect to intellectual property to publication, including the timing of publication, with respect to intellectual property. In so doing we confirm that we have followed the regulations of our institution intellectual property.

We understand that the Corresponding Author is the sole contact for the Editorial process (including Editorial Manager and direct communications with the office). He is responsible for communicating with the other authors about the progress, submissions of revisions and final approval of poofs. We confirm that we have provided a current, correct E-mail address which is accessible by the Corresponding Author and which has been configured to accept E-mail from [Tangchaoke@qq.com](mailto:Tangchaoke@qq.com).

Signed by all authors as follows:

Zhen-wang Zhao, Min Zhang, Jin Zou, Xiang-Jun Wan, Li Zhou, Yao Wu  
Shang-ming Liu, Jing-xiao Zhao, Heng Li, Yu-sheng Qin, Xiao-Hua Yu, Chaoké Tang

**Declaration of interests**

The authors declare that they have no known competing financial interests or personal relationships that could have appeared to influence the work reported in this paper.

The authors declare the following financial interests/personal relationships which may be considered as potential competing interests:

Journal Pre-proof